

We are IntechOpen, the world's leading publisher of Open Access books Built by scientists, for scientists

4,800

Open access books available

122,000

International authors and editors

135M

Downloads

Our authors are among the

154

Countries delivered to

TOP 1%

most cited scientists

12.2%

Contributors from top 500 universities

**WEB OF SCIENCE™**Selection of our books indexed in the Book Citation Index
in Web of Science™ Core Collection (BKCI)

Interested in publishing with us? Contact book.department@intechopen.com

Numbers displayed above are based on latest data collected.

For more information visit www.intechopen.com

Design and Fabrication of Printed DNA Droplets Arrangement and Detection Inkjet System

Jian-Chiun Liou

Additional information is available at the end of the chapter

<http://dx.doi.org/10.5772/63329>

Abstract

This article describes the aims to establish a thermal bubble printhead with simultaneously driving multi-channel for DNA droplet arrangement. It proposed a monolithic CMOS/MEMS system with multi-level output voltage ESD protection system for protected inkjet printhead. High-voltage power, low-voltage logic, and CMOS/MEMS architecture were integrated in inkjet chip. It used bulk micromachining technology (MEMS). On-chip high-voltage electrostatic discharge (HV-ESD), protection design in smart power technology of monolithic inkjet chip is a challenging issue. The nozzle jets interleaving scanning sequence is controlled spatially on the elements to avoid the strong interference with DNA droplets caused by the excitation of the neighbor driven elements. A heating element, disposed on the substrate, includes a conductor loop which does not encompass the heating elements on the substrate. The configuration of the heater jet significantly reduces both electromagnetic and capacitance interference caused by the heating elements. The simulation and experience result have shown in the research. It is reduced nearly half the time compared to the case with traditional scanning sequence. This experiment develops new controlled structure designs of chip for inkjet printheads. A bubble inkjet(TIJ) device is designed, several of the architectures may be adjusted just a small microns to improve and optimize the DNA drop nucleation and generation efficiency. The DNA droplet ejection behavior of the multiplexer inkjet printhead within 60- μm orifice size has been measured beyond 5 kHz operation system, 12 pL capacity of ejected DNA droplet volume.

Keywords: DNA droplets, CMOS/MEMS, addressing

1. Introduction

An intelligence inkjet printhead includes a number of heater and nozzle devices formed on a silicon substrate. For reliable operation of the jet heater in a practical thermal ink-jet printhead chip [1–10], external sources of noise become an extremely important concern. It is desirable that the jet heater be disposed on the chip at a location as close as possible to the channels themselves for a most accurate reading of the actual temperature of the liquid ink just before a given ejector is fired. At the same time, the location of the jet heater must be rigorous designed because an additional requirement of a experiential bubble jet printhead is that the chip be as small as physically possible, yet still contain all the circuits required for valid operation [11–16].

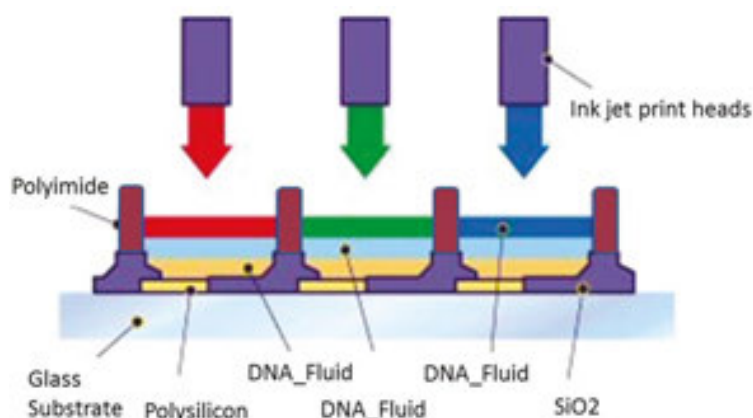


Figure 1. Inkjet printer heads system and multi-channel printhead jets.

The DNA droplet ejection of our addressing N bits jets elements switch multiplexer circuit system printhead has been measured of ejected DNA droplet behavior. There is up to 1024 and even a larger number of elements for a variety of printhead nozzle examinations. The jets interference and the power consumption for such a high-density system, however, make it difficult to achieve a high printing speed, low cost, economic, high-performance, and high-resolution device. In order to alleviate the low noise interference and low-power requirement of jets, a high-voltage driver and logic multiplexer are nowadays employed to match each nozzle of the printhead jet elements and therefore improves the printhead's overall power dissipation. **Figure 1** shows inkjet printer heads system and multi-channel printhead jets using novel encoding algorithm system. Addressing N bits jets elements switch circuit system is using in inkjet chip. Logic functions integrated, enabling TIJ-based products have become increasingly high-end market [17–23]. Inkjet printers can put small number of DNA droplets (usually only a few picoliters, 10–12 l) accurately sprayed on to DNA glasses media. Integrated circuit of the TIJ described transducer array to provide the 1024 ejection jets, includes a data interface, an DNA ink-jet treatment, short-pulse generation, and bidirectional method operation. The chip system also has an output function to manage of multi-chip electronic components into larger arrays. TIJ spray hole array chip design architecture allows less than

10 input lines of addressing 1024 nozzles. **Figure 2** shows printed DNA droplets “AGCT” arrangement and detection.

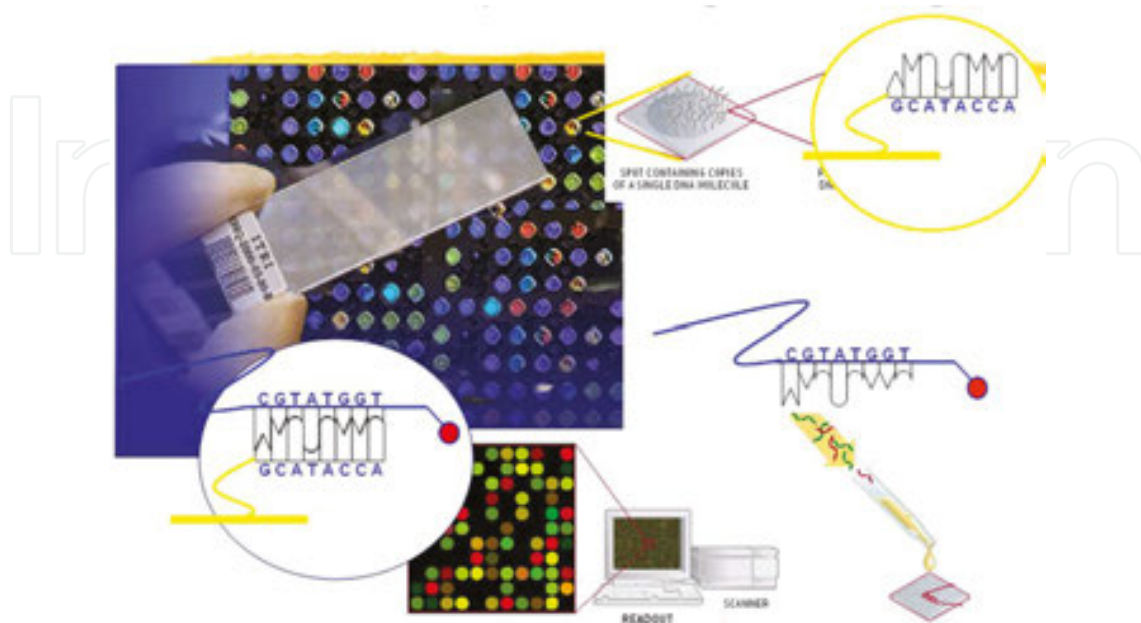


Figure 2. Printed DNA droplets “AGCT” arrangement and detection.

Human birth, old age, sickness and death process, and cellular changes are related to changes in the cell and turn machine in the DNA have been around for a round to be free from the disease, prevent aging dream, universally invested considerable manpower material, and finally solved the mystery of the human DNA code. However, the cause of the test, the correct dosage, and even tailored drugs are dependent on fast, accurate, simple, and inexpensive test technology.

Traditional testing methods, slow and time-consuming, difficult to control the accuracy and cost is very high, limiting the rapid development of biomedical science. Use Biomedical MEMS and microfluidic system technology developed in the biomedical wafer, for DNA sequencing, testing, screening, and development of new drugs, quantitative release of the drug, as well as food, environmental testing and other diseases, to provide a fast, accurate, large, and automation platform. I believe will be able to promote the development of the next stage of biotechnology, provide a degree of contribution.

Biomedical wafer has to do trace detection, quantitative precision, automation, and fast parallel processing, and many other advantages, compared with the traditional biomedical detection, have tremendous advantages, and so far, it has also been a lot of breakthrough technological developments. But it must be said, biomedical wafer also faces many technical challenges, by scientists in different fields need to be overcome. The use of high-density microfluidic device similar to a color inkjet printer's thermal bubble inkjet and other key technologies, each has independent probe of the trace liquid tank, pipeline microfluidics, liquid discharge hole. Trace



Figure 3. Ejection chamber (firing chamber) and cavity geometry shapes.

each liquid tank filling oligonucleotide, after large pieces of DNA probe solution or sugars, can be more than one million droplets ejection.

We use liquid jetting method in addressing the DNA on the slide; it is a precise and rapid deployment of quantitative methods. Generating and physical aspects of the process model simulation of heat dissipated in the growing bubble. It is used thermal bubble nucleation theory (bubble nucleation theory) to simulate the physical mechanism of heat generated by the bubble. It is to discuss ejection chamber (firing chamber) and cavity geometry shapes to reach backfill mechanism of DNA as shown in **Figure 3**. Calculation procedure thermal bubble jet pump decline is a fluid field problem free surface, while the shape of the free surface of the flow field will change with those changes, so to understand the characteristics of injection, must respect the free surface Discussion of issues to be studied.

Numerical simulation of a need to calculate immiscible dominated by the surface tension of the free liquid surface control (free surface). This free surface on both sides and the physical properties of the fluid pressure has discontinuous nature of change; computer simulation program is the key to success lies in tracking the exact location of this discontinuous liquid level.

2. Single channel calculated injection cavity design of the simulation

Computer simulation is the traditional type of single channel for supplying a fluid ejection chamber (firing chamber) simulation. Injection cavity geometry is shown in **Figure 4**. Orifice diameter of $60\ \mu\text{m}$, the thickness of the orifice sheet is $50\ \mu\text{m}$, dry film thickness of $60\ \mu\text{m}$, the bottom area of the injection chamber is $120\ \mu\text{m} \times 120\ \mu\text{m}$, the area of the heater was $105\ \mu\text{m} \times 105\ \mu\text{m}$. **Figure 5** calculated result is for the injected fluid which is water to 5 kHz operating frequency, and the three-dimensional side view of a two-dimensional cross-sectional view in the XZ 10, 20, 30, 40, and 200 μs injection case.

Computer simulation is still the traditional type in a single passage of the fluid supplied to the injector chamber to simulate. **Figure 6** calculated result is for the injected fluid which is changed to DNA. It is 5 kHz operating frequency, three-dimensional, and three-dimensional side view view at 10, 20, 30, 40, and 200 μs injection scenario. Single-channel injection cavity is not for Z-axis direction completely symmetrical design. It is a droplet drag tail vulnerable asymmetrical flow field forces. It makes the deflection direction of flight. On a three-dimensional view,

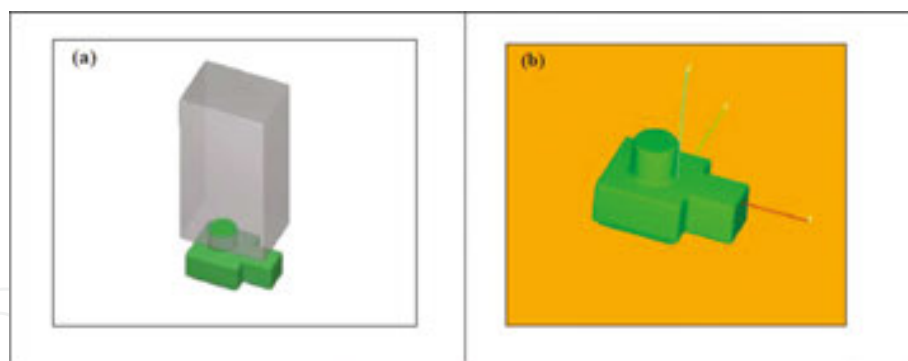


Figure 4. Computer simulation created by (a) calculation of regional, (b) three-dimensional map of the microfluidic single channel.

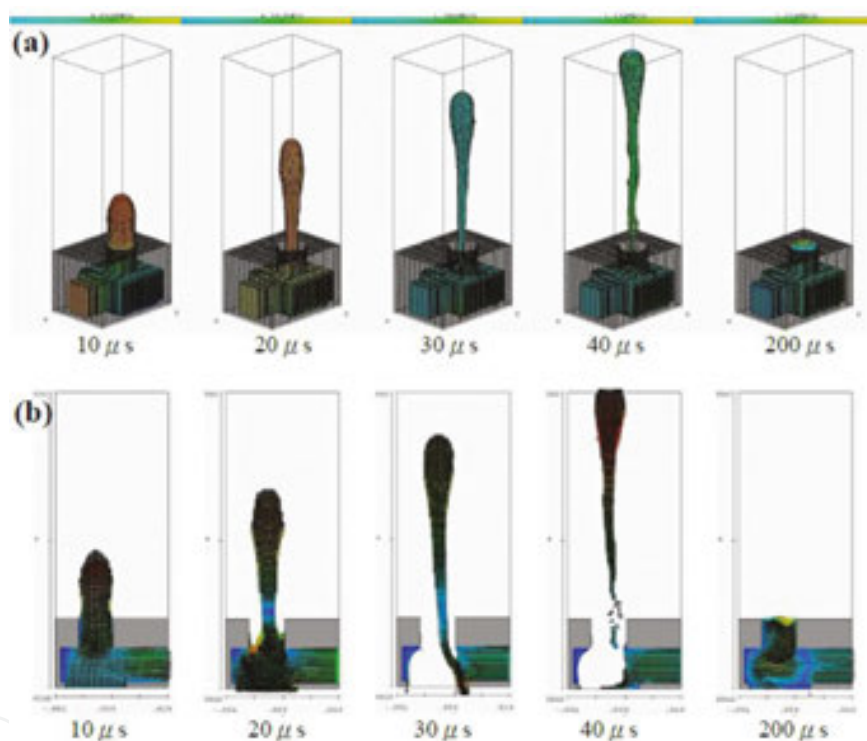


Figure 5. Computer simulation of water in the nozzle diameter $60\ \mu\text{m}$ and $50\ \mu\text{m}$ thickness of a single channel injection cavity, an operating frequency of $5\ \text{kHz}$, in (a) a three-dimensional side view (b) XZ sectional view of a two-dimensional, 10 , 20 , 30 , 40 and $200\ \mu\text{s}$ injection scenario.

it can be seen clearly. The fluid is water or gasoline, because both the geometry of the cavity injection asymmetry makes the tail dragging flight direction deflection. **Figure 7** for the two-dimensional calculation results X–Z sectional view. X–Z sectional view of the results in $200\ \mu\text{s}$ moment, we can see that the liquid level of the fluid, although not yet fully reached the nozzle exit, but DNA is still almost complete backfill. The results also show the geometry of this injection cavity design, operating at a frequency of $5\ \text{kHz}$ for, in terms of the DNA is the upper limit of the operating frequency. To further increase, the operating frequency may be less than

the ink supply phenomenon. **Figure 8** is compared with two-dimensional flow field inside the internal cavity of the injection X–Y sectional view of the results. It is the internal flow field vector and water, as shown in below. It is not much difference, showing backfill speed slower than the water.

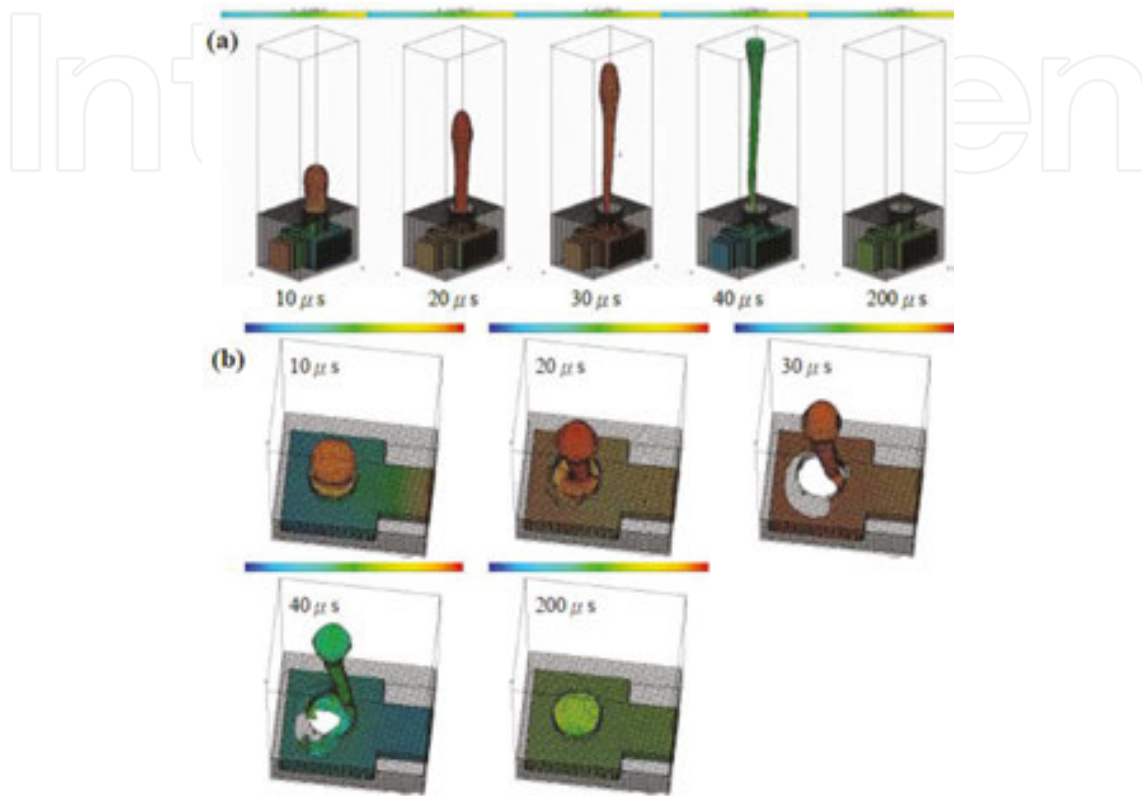


Figure 6. Numerical simulation of DNA in the nozzle diameter 60 μm and 50 μm thickness single-channel injection cavity to 5 kHz operating frequency, to (a) a three-dimensional side view (b) on a three-dimensional view, 10, 20, 30, 40 and 200 μs of injection scenario.

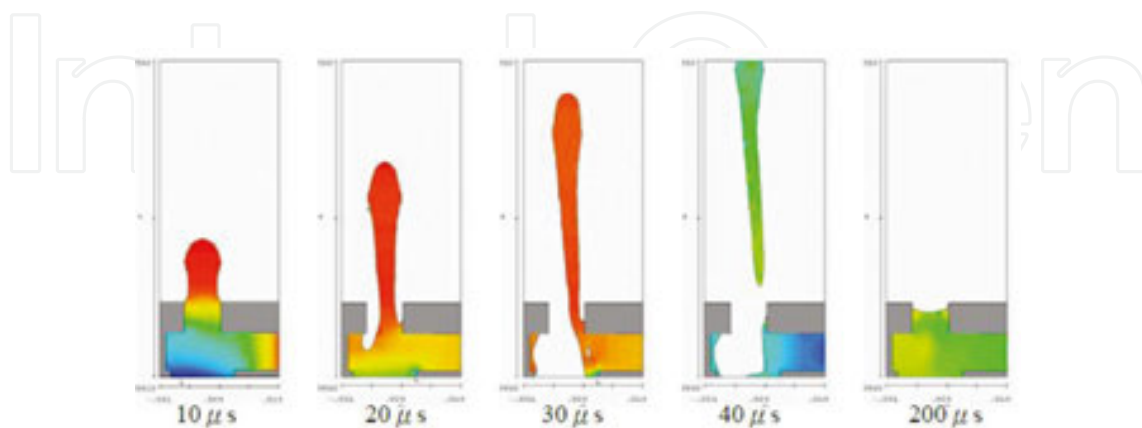


Figure 7. DNA computer simulation in the nozzle diameter 60 μm and 50 μm thickness of a single channel injection cavity to 5 kHz operating frequency, in the two-dimensional X–Z sectional view, at 10, 20, 30, 40 and 200 μs injection scenario.

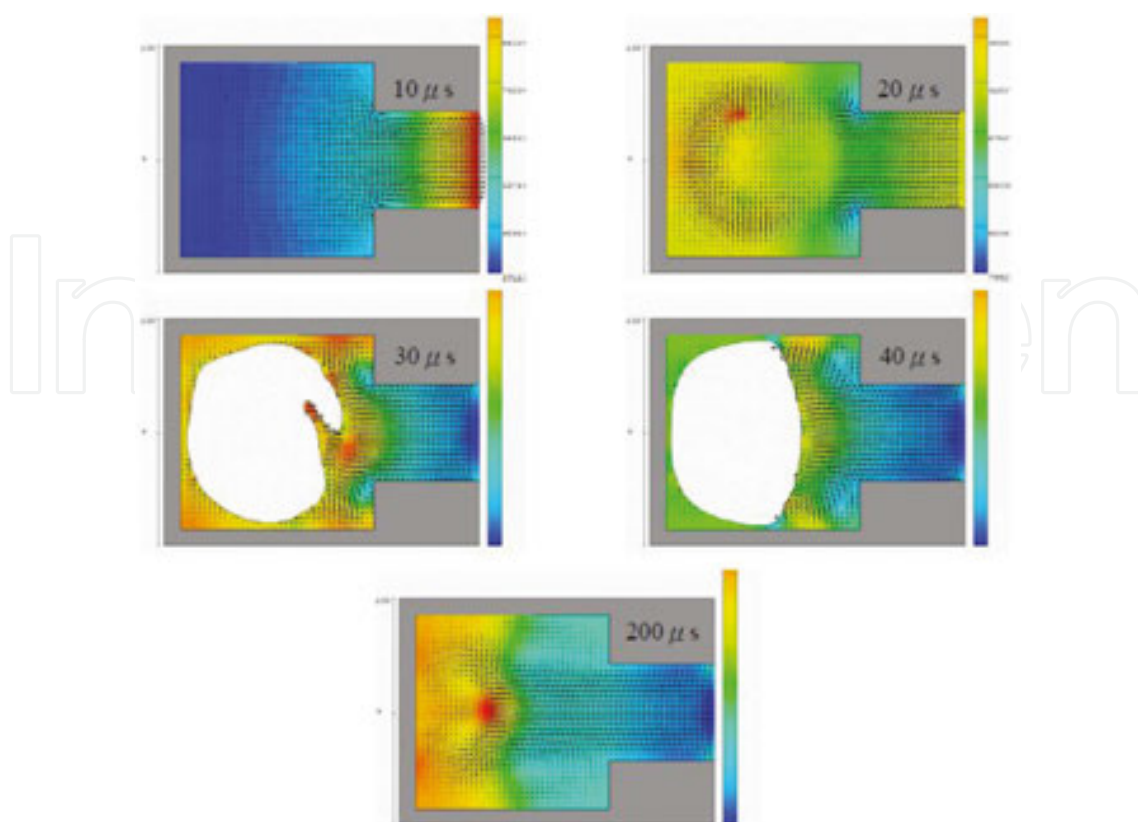


Figure 8. Numerical simulation of DNA in the nozzle diameter $60\ \mu\text{m}$ and $50\ \mu\text{m}$ thickness of the single-aisle jet cavity to $5\ \text{kHz}$ operating frequency, the X-Y two-dimensional cross-sectional view, in 10 , 20 , 30 , 40 and $200\ \mu\text{s}$ injection scenario.

It is at the same voltage, the heating time, and other conditions. Because different working fluids (water and DNA), and for the same single injection but may result in different maximum flow. The cause of this problem, there are two possible reasons, the first is due to the poor design of single microfluidic channel, resulting in the flow of work done when the thermal bubble jet DNA monomer heater inlet to the push-back is greater than the flow path to the nozzle holes the launch of the top jet fuel. Thus, causing loss affects a large number of heater acting DNA spray flow. At the same time, due to differences in the physical properties of DNA and water, so that the DNA greater than water leakage, resulting in a smaller flow nozzle exit. Narrowing the channel inlet cross-sectional area is a method you can try, but this method also simultaneously increase the time required for DNA backfilling injection chamber, the monomer jet ejection frequency may therefore need to fall. In addition, since the monomer jet DNA to reduce the cooling effect is reduced, so cause DNA monomer generates heat accumulation effect and affect the efficiency of DNA spray, spray a vicious cycle that causes DNA not been apparent efficiency. Another possibility is due to the thermodynamic properties of water and DNA in the table. Temperature, the vertex (critical point) of the magnitude of the pressure is not the same. Even under the same operating conditions of voltage and time of heating, the heat generated bubble internal pressure is not the same size, that is, have different sizes of thrust. Thermal bubble pressure and water produced large thrust, the jet and the flow rate is also larger. In the same function and the same thrust geometric shape of micro-channel design,

the simulation by calculation, preliminary verification can launch jet monomer droplets, the difference volume flow (volume flux) of. Release of DNA volumetric flow rate is relatively low, due to the different physical properties of DNA inference with water, causing DNA to the channel inlet neck (neck channel entrance) the loss is greater than the flow rate of water flow loss. **Figure 9** is the volumetric flow rate of the working fluid through the top of the water and the DNA cross-sectional area of the calculated change with time in figure. This showed that both the volumetric flow rate is not much difference with the total volume of traffic resulting time integration. The inference from the above calculation results under the same operating conditions, hot water bubble pressure, and thrust generated by comparing DNA large, resulting in the ejection of the flow is also larger.

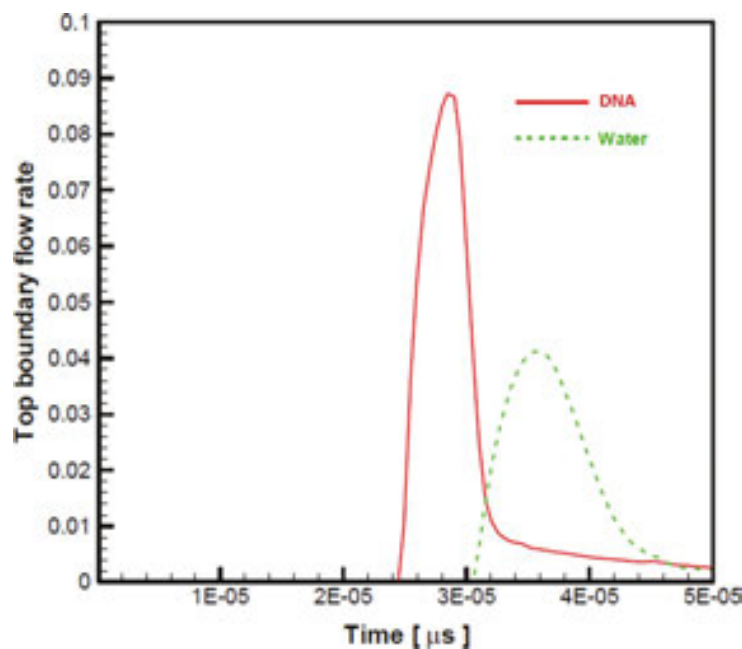


Figure 9. Volumetric flow rate of water through the top and DNA computing sectional area of change with time of the case.

A method for increasing the injection flow rate, in addition to increasing the frequency of injection outside, increasing the ejection orifice diameter of the cavity is also a method to try. But may have other negative effects such as fluid leakage orifice is easy to form puddles (puddling), the need for evaluation by computer simulation verification, in order to determine the negative impact is not the whole jetting performance. **Figure 10** evaluates to the orifice diameters ranging from 60 μm increased to 80 μm, when the injected fluid remains gasoline to 5 kHz ejection frequency, three-dimensional and three-dimensional side view at 10, 20, 30, 40, and 200 μs in the case of injection. With the results shown in **Figure 10**, comparison can be learned in the same circumstances thrust function, because the spray hole diameter increases, so the ejected droplet volume increases. In 40 μs results instantly show droplet flying speed quite significantly reduced. It is produced a relatively large volume of satellites and flying very slowly. **Figure 11** for the two-dimensional calculation results XZ section; at the moment of 40 μs results showed, as exports slow so that the droplet is not out of the nozzle holes with

respect to the results in **Figure 10** for spray when the hole is 60 μm , in an instant 40 μs , the droplet tail is already out of the nozzle holes. **Figure 12** is the result of the calculation of the X–Y two-dimensional section, due to the increase in the spray orifice diameter, relatively large volumes of a spray of droplets. In the cross-sectional area of the flow path, inlet same circumstances take longer to completely fill the internal cavity of the injection orifice until the surface, while the inner flow field to stabilize. Internal flow velocity vector field is still supplying single-channel direction of the fluid toward the discharge chamber in the direction of the moment of 200 μs .

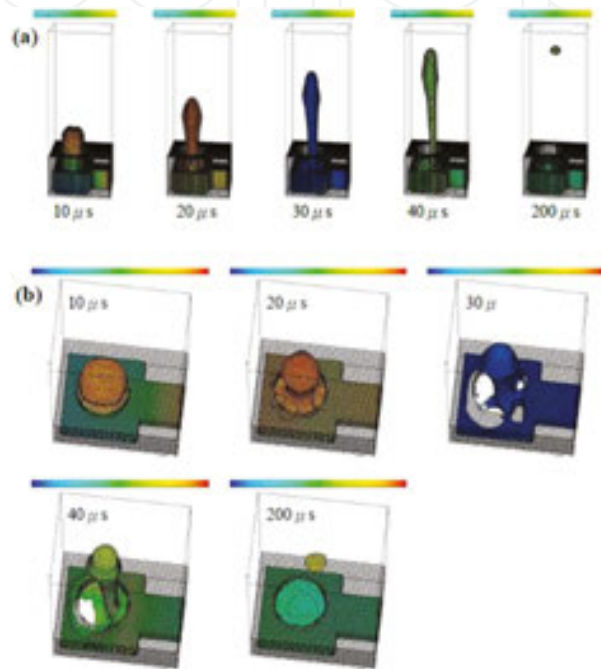


Figure 10. Numerical simulation of DNA in the nozzle diameter 80 μm and 50 μm thickness single-channel injection cavity to 5 kHz operating frequency, to (a) a three-dimensional side view (b) on a three-dimensional view, 10, 20, 30, 40 and 200 μs of injection scenario.

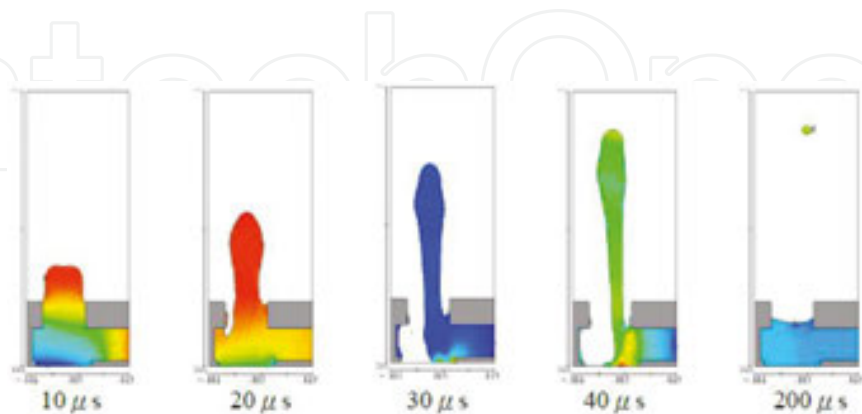


Figure 11. DNA computer simulation in the nozzle diameter 80 μm and 50 μm thickness of a single channel injection cavity to 5 kHz operating frequency, in the two-dimensional X–Z sectional view, at 10, 20, 30, 40 and 200 μs injection scenario.

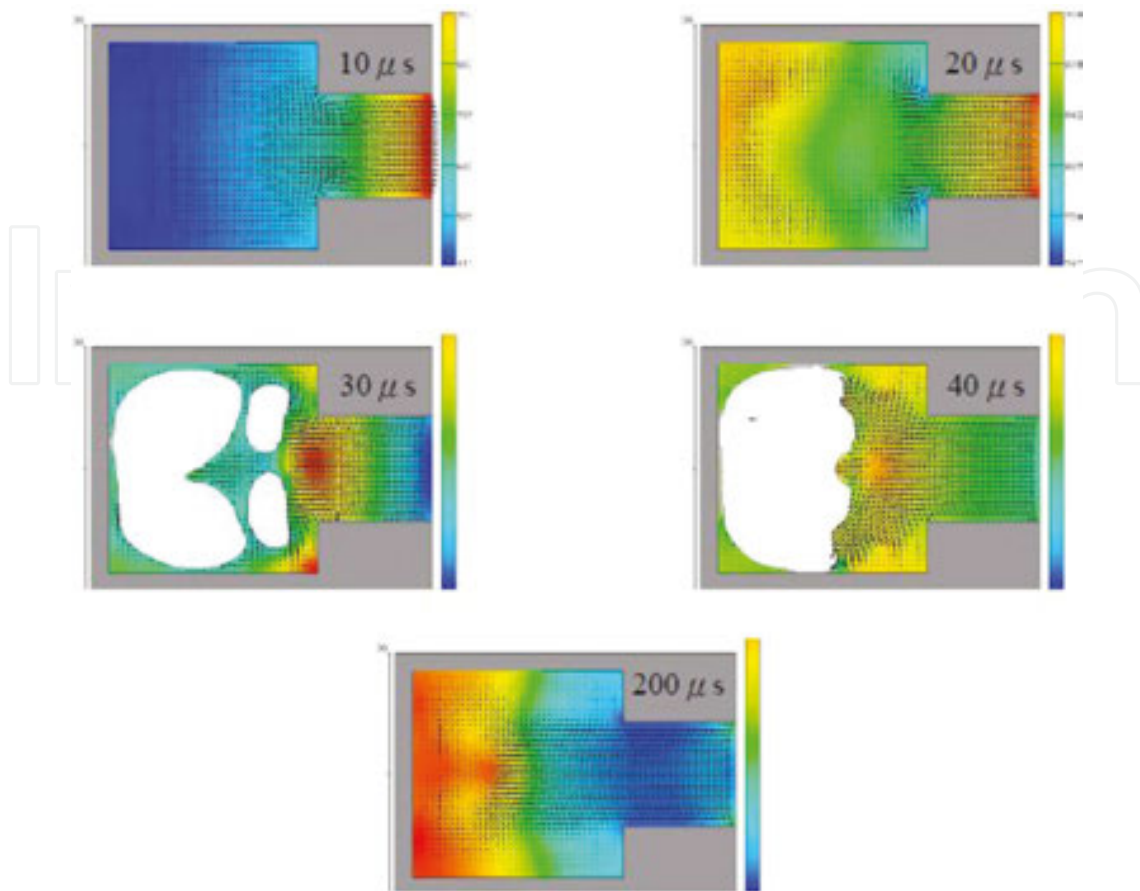


Figure 12. Numerical simulation of DNA in the nozzle diameter $80\ \mu\text{m}$ and $50\ \mu\text{m}$ thickness of the single-aisle jet cavity to $5\ \text{kHz}$ operating frequency, the X–Y two-dimensional cross-sectional view, in 10 , 20 , 30 , 40 and $200\ \mu\text{s}$ injection scenario.

Increase the injection flow rate of the other direction of thinking in order to increase the volume inside the cavity injection, in order to that the injected volume of the droplet can be increased, so the study also hope that through computer simulation to verify its feasibility. **Figure 13** for the calculation of simulated gasoline nozzle diameter and $60\ \mu\text{m}$ thickness of $50\ \mu\text{m}$, dry film (dry film layer) increases the height by $60\ \mu\text{m}$ to $90\ \mu\text{m}$ single-aisle jet chamber, which internal cavity volume 150% increases in operating frequency of $5\ \text{kHz}$, XZ dimensional, three-dimensional side view, and sectional view, in 10 , 20 , 30 , 40 , and $200\ \mu\text{s}$ in the case of injection. The result of the calculation shows that the droplet flying speed and directivity of **Figures 3–12** dry film $60\ \mu\text{m}$ when the height of the result is not much difference, but when $40\ \mu\text{s}$ has been out of the spray droplets hole; but $200\ \mu\text{s}$ instantaneous results show that the fluid has reached the finish filling orifice surface, while the overflow orifice phenomenon is easy to form puddles phenomenon. Therefore, increasing the height of the dry film that is to increase the volume inside the cavity injection, although you can increase the flow rate of backfill raise, it is still possible because the backfill too fast, and out of the orifice puddles formed on the surface of the phenomenon, probably because last fluid left in the orifice surface, so that subsequent ejection of a droplet directionality poor is to increase the dry film thickness may be required to pay attention to the negative effects derived.

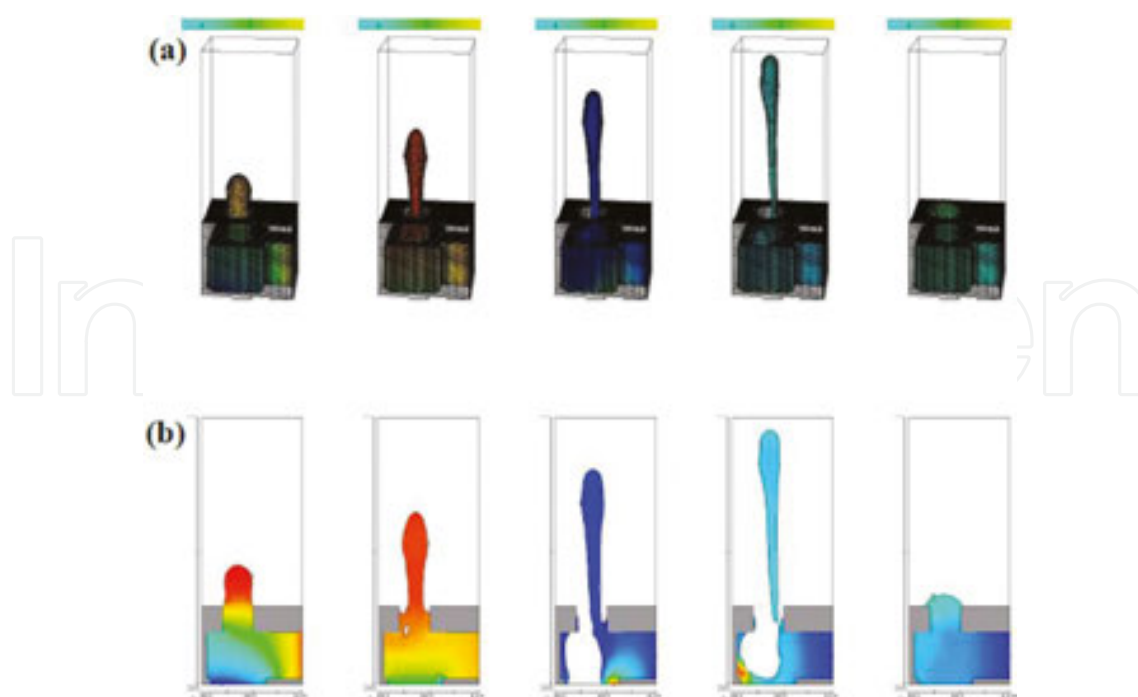


Figure 13. DNA computer simulation in the nozzle diameter $60\ \mu\text{m}$ and a thickness of $50\ \mu\text{m}$, a height of $90\ \mu\text{m}$ dry film of the single-channel injection cavity, an operating frequency of $5\ \text{kHz}$, in (a) a three-dimensional side view (b) XZ sectional view of a two-dimensional, in $10, 20, 30, 40$ and $200\ \mu\text{s}$ injection scenario.

3. Dual-tapered calculated injection cavity design of the simulation

It is an injection operation in various applications nozzle (ink jet head). It is a special microfluidic flow channel structure. Backfill fluid injection and two complementary action this period, to be injected fluid within the microfluidic flow path ilk field direction opposite directions. This phenomenon will seriously affect the speed of the fluid backfill supplement and seriously affect the operation frequency of jets. From the simulation result, the system is to solve the problem of liquid flow. It is a dual-type injection cavity design having a fluid passage. At the same time, the fluid has a single-flow direction. It is to reduce the resistance of the fluid, shortening the filling time of the fluid. It is possible to increase the operating frequency of the monomer injection, thereby increasing the maximum injection flow rate.

In this study, it is the geometry and design by microfluidic flow channel. It is a single-direction flow velocity field compared to the entire cycle of backfill fluid flow direction. Therefore, it is to enhance its complement backfill fluid velocity. When the nozzle operating frequency increases, the fluid flow to replenish backfill required for stabilization of fluid ejection chamber fluid level backfill added time will dominate the operating frequency of the jets. Therefore, reducing the time to replenish the fluid needed for backfill will greatly enhance the operating frequency of the jets. Since the droplet ejection but also take away a lot of heat generated by the water heater, a considerable cooling effect reduces the internal temperature of the wafer. So there is also always a considerable improvement in the service life of the wafer. To achieve



Figure 14. Computer simulation created by (a) calculation of regional scope, (b) a tapered three-dimensional map of the dual-channel microfluidic.



Figure 15. Numerical simulation of DNA in the nozzle diameter $30\ \mu\text{m}$ and $50\ \mu\text{m}$ thickness tapered dual channel injection chamber to $10\ \text{kHz}$ operating frequency, three-dimensional side view, in $10, 20, 30, 40, 100, 110, 120, 130,$ injection of the case 140 and $200\ \mu\text{s}$.

the above purpose, it is designed to spray a tapered cavity structure of dual-channel microfluidic. **Figure 14** is the three-dimensional microfluidic tapered dual-channel region of a perspective view of the computing range. This type of gradual reduction for dual-channel microfluidic injection chamber numerical simulation conducted to assess the effectiveness of its injection. **Figure 15** for DNA to orifice diameter $30\ \mu\text{m}$ and $50\ \mu\text{m}$ thickness tapered dual-channel injection chamber to $10\ \text{kHz}$ operating frequency, three-dimensional side view of $10, 20, 30, 40, 100, 110, 120, 130, 140,$ and $200\ \mu\text{s}$ injection scenario. $110, 120, 130, 140,$ and $200\ \mu\text{s}$ belong to second injection stage. **Figure 16** is compared to the two-dimensional X–Y sectional view, in the case of injection $10, 20, 30, 40, 100, 110, 120, 130, 140,$ and $200\ \mu\text{s}$.

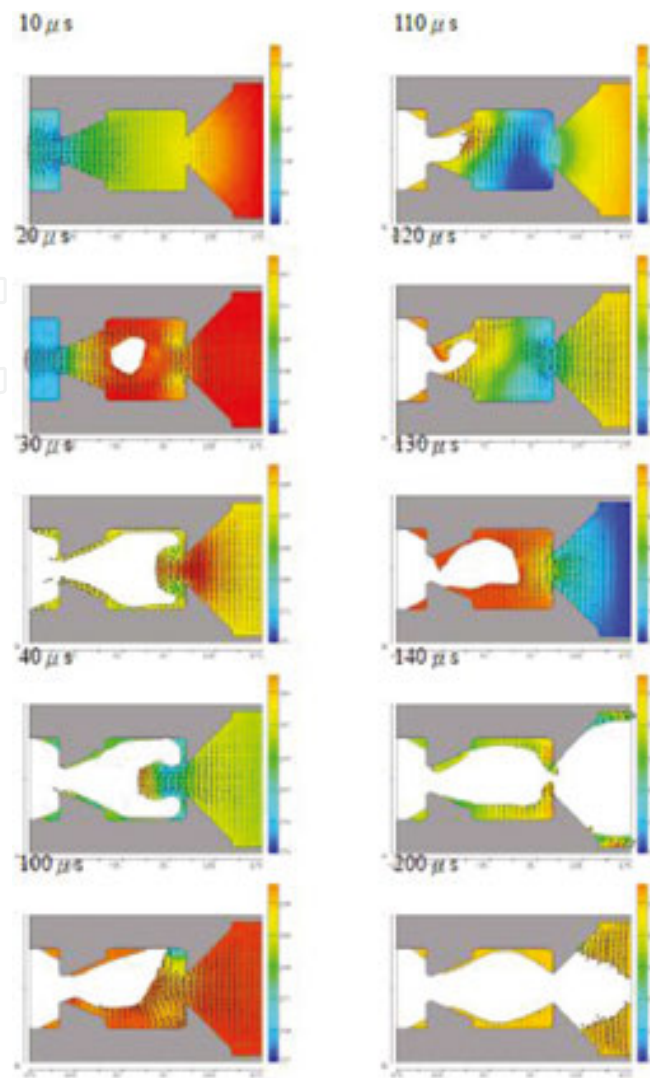


Figure 16. Numerical simulation of DNA in the nozzle diameter 30 μm and 50 μm thickness tapered dual channel injection chamber to 10 kHz operating frequency, the XY two-dimensional cross-sectional view, in 10, 20, 30, 40, 100, 110, 120, injection case 130, and 140 of 200 μs .

The XY two-dimensional cross-sectional view shows that the internal flow field this injection cavity does not have the speed of the flow field in a single direction, so it becomes counter-flow injection of small, but the volume of the second droplet ejection seems to be more for the first time the injection volume is slightly larger. The reason may be due to the tapered microfluidic injection chamber at the start of the two-channel state under stationary conditions. When the first injection, the injection inside the cavity and cannot be achieved immediately single-flow velocity flow field. It requires a certain number of jet action, or the need to increase the flow path style tapered angle, have a chance to achieve a single direction of flow velocity field.

Figure 17 is the result of the calculation of the initial conditions set for the injection inside the cavity has a single-class field direction of situations. DNA double-tapered channel in the injection chamber to 5 kHz operating frequency, three-dimensional and three-dimensional

side view on view at 10, 20, 30, 40 and 50 μs injection scenario. From the results shown that the results of the droplet ejection volume comparing **Figure 16**. There is an increasing convergence of big. Results indicate if the ejection velocity flow field inside the cavity having a single direction of the flow field. It is the ejection of flow convergence increase, while reducing the time required for the fluid filling the cavity of the injection, but also to simultaneously increase the ejection frequency. **Figure 18** is compared with the two-dimensional X–Y sectional view at 10, 20, 30, 40 and 50 μs injection scenario.

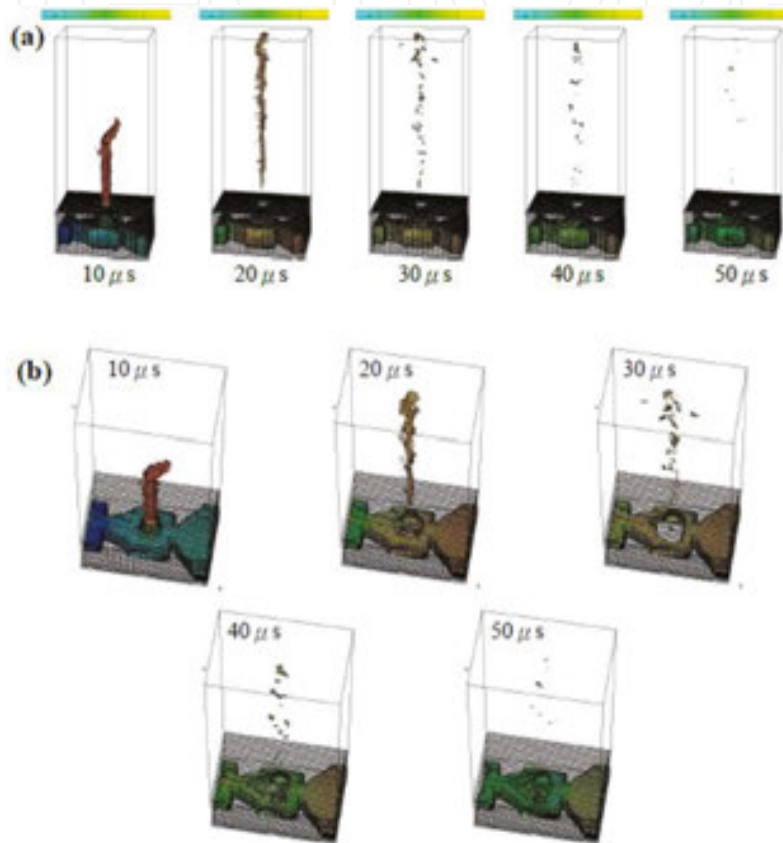


Figure 17. Numerical simulation of DNA in the nozzle diameter 30 μm thickness and tapered dual channel injection cavity 50 μm to 5 kHz operating frequency, to (a) a three-dimensional side view (b) on a three-dimensional view, 10, 20, 30, 40 and 50 μs injection case.

Because of the time course of planning this program, yet there is enough time for this can be tapered dual channel injection chamber, do computer simulation analyzes of various design parameters such as the angle of the tapered flow channel type, respectively to be few degrees preferred design. Application of the heater to produce instant hot bubble of high pressure jet thrust derived monomer. While allowing fluid flow velocity has a single field. Ejection frequency can be increased, and thus get the most traffic. It is currently unable to give details of the desired design dimensions apply to this program the best dual-channel injection tapered cavity to obtain maximum injection efficiency. Continue to be the future of the current simulation analysis to identify micro-injection monomer flow path design can operate at high operating frequencies.

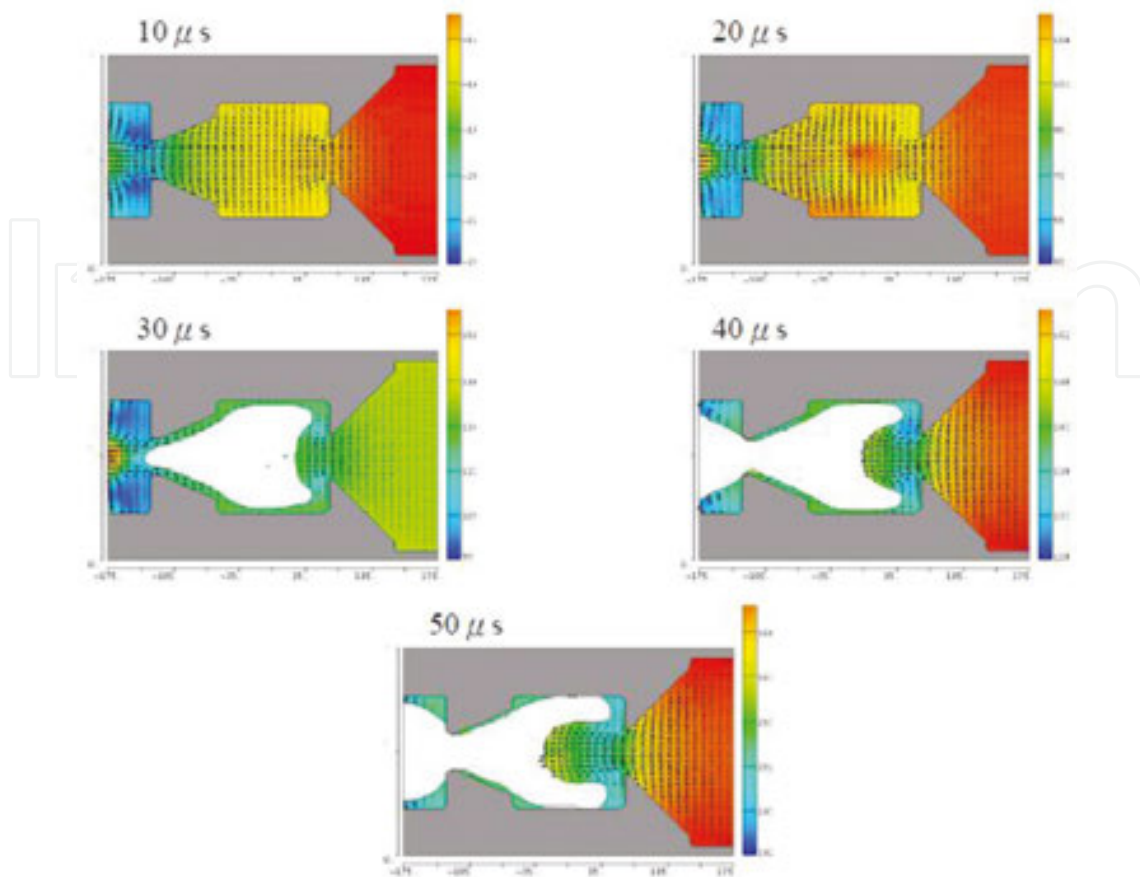


Figure 18. Numerical simulation of DNA in the nozzle diameter 30 μm thickness and tapered dual channel injection cavity 50 μm to 5 kHz operating frequency, the X-Y two-dimensional cross-sectional view, in 10, 20, 30, 40 and 50 μs injection case.

Printing method is the change comes from an inkjet printer, with the heated bubble manner nucleic acid probe is placed on a glass slide using a gene chip production to 30,000 points as shown in **Figure 19**.

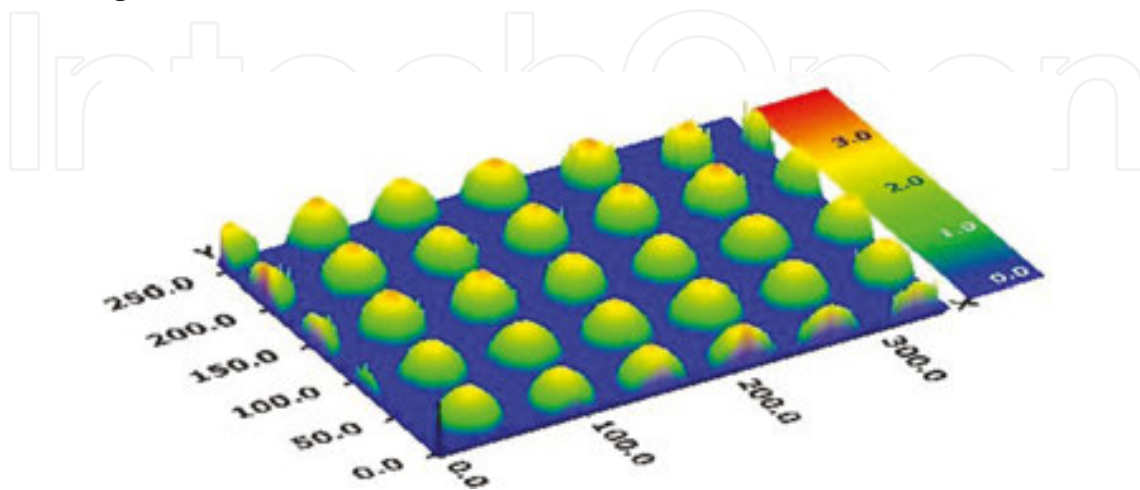


Figure 19. DNA droplets profile.

4. Printed DNA droplets arrangement and detection

Situ synthesis (in situ synthesised), the nucleotide sequence of molecules by using different methodologies to control chemical reactions forming a jieshangqu a nucleic acid sequence, the rapid production of precision (accurate positioning and orientation uniform), ultra-high density (1 million–200 million points) wafer. Synthesis There are two kinds, one is the use of liquid jet technology, such as nucleotide-like ink injected into a specific location subjected to solid phase synthesis (solid phase phosphoramidite chemistry). The whole chip layout is show in **Figure 20**.

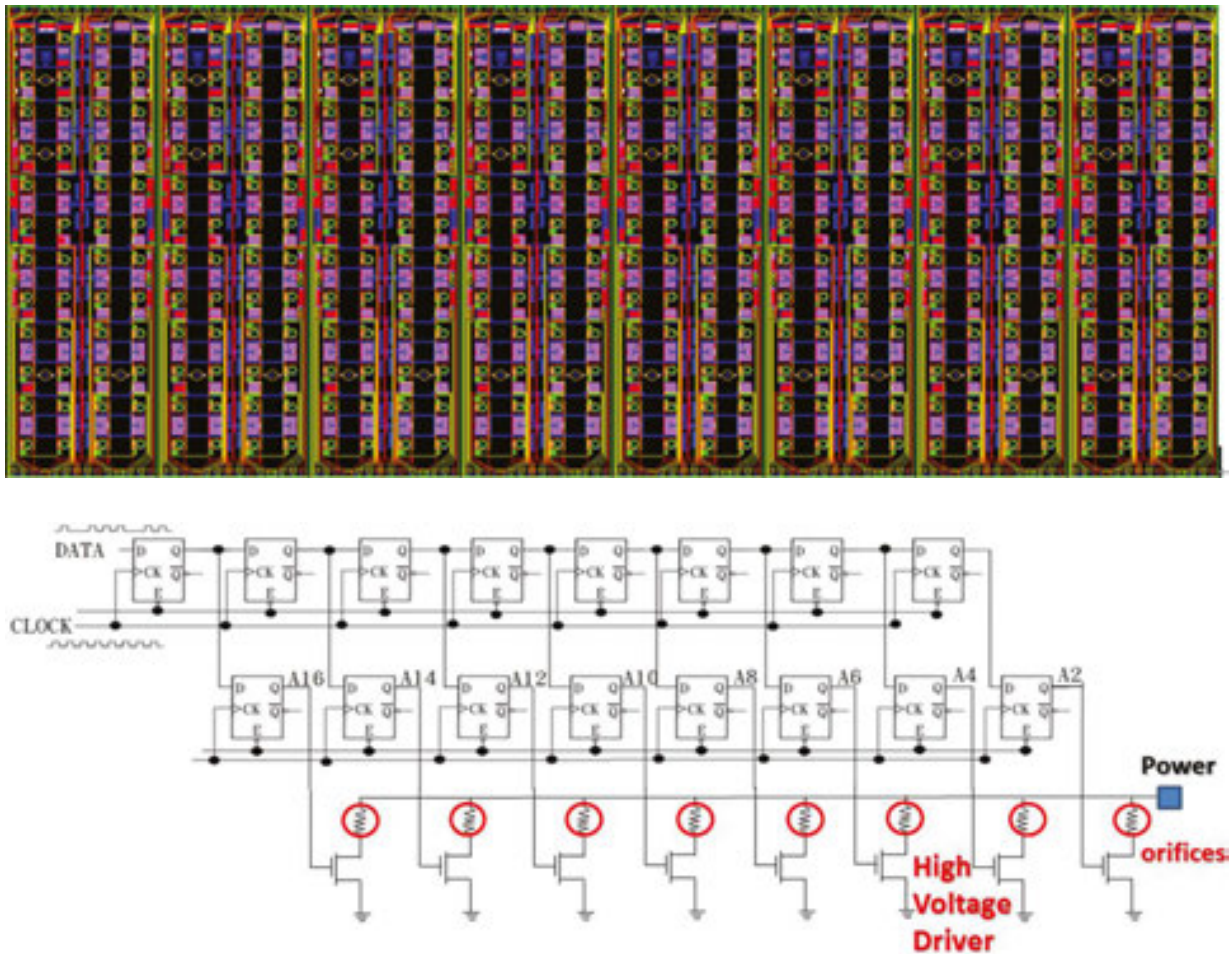


Figure 20. (a) The whole chip layout. (b) The detail circuit(DFF) diagram of chip.

System is to determine a DNA liquid printed head with two hundred orifices, each orifice to orifice distance is another 2000 μm . It is to select the drive mode, respectively, following several ways. The first is the direct voltage direct drive via Pad on the wafer, the drawback is the number of multi-Pad. The second drive element is a driving thin-film resistance element. It is the driving element has a variety of points. It is the n-type metal-oxide half effect transistor factory.

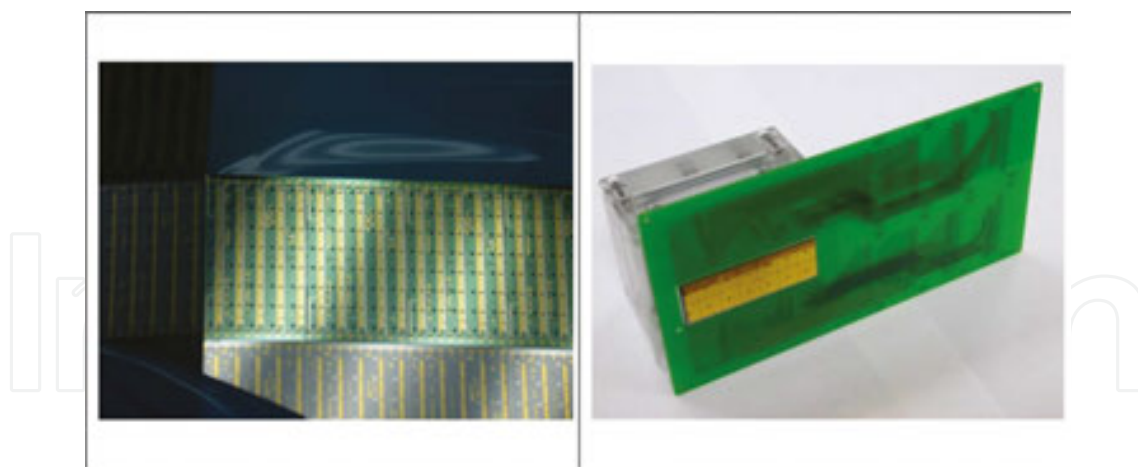


Figure 21. DNA droplet chip and module.

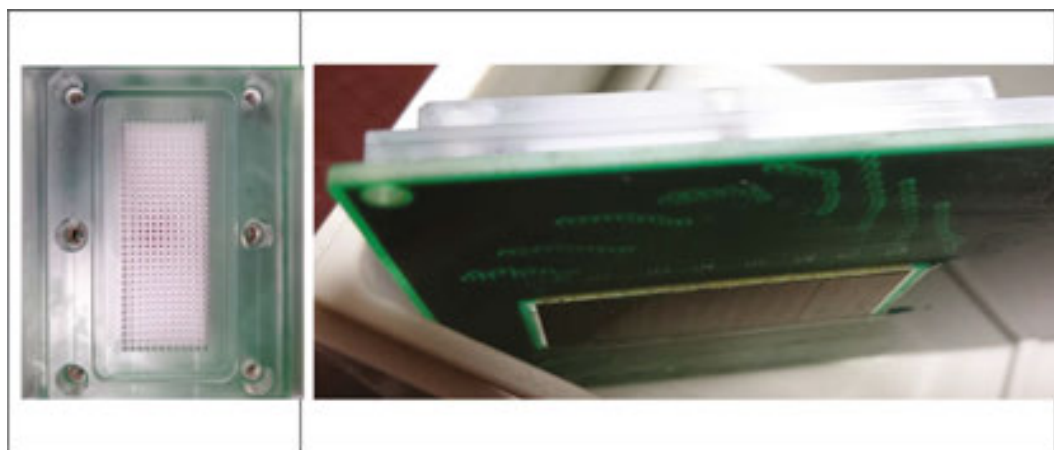


Figure 22. Multiplexer DNA solution jet part.

It is the use of an n-type metal-oxide semiconductor transistor to drive a thermal film. It is the thermal resistance of the film due to the long drive driving the heat bubble reagent sprayed onto glass slides. Taking into account the upper and lower symmetrical design of the wafer, so we must first decide with each other and each of the driving elements thin-film resistance elements are arranged. It is the liquid discharge head of the wafer area is very large. We design each wafer map 384 orifices as shown in **Figure 20a**. Our first idea is to spray the wafer to contact aligner way DNA production. The entire wafer is DFF(D-Flip-Flop) data staging operation and high-voltage driver circuit as shown in **Figure 20b**. This circuit can be applied to one or more of the control input signal to change the state, and there will be one or two outputs. Flip-flop is the basic logic unit is configured to sequence logic circuit and a variety of complex digital systems. Flip-flops and latches are essential components used in computer, communications and many other types of systems in the digital electronic systems.

Integrated spray liquid infusion tube sheet and the card brake package as shown in **Figures 21 and 22**. It is the result of a special liquid jet architecture DNA cloth into the slide.

Since microarray dataset wafer has a very large number of the number of genes. It is based on grouping method to automatically discover biological modules (biological modules) is an important theme of the microarray chip analysis. It is a functional grouping (functional Clustering). It is a common occurrence frequency by corresponding functional gene annotations (functional annotation) between (co-occurrences) measurements for clustering. So it can make related genes and annotations easy reach of digital analysis to facilitate the subsequent establishment of the assumptions and experimental design.

The core principles behind the array hybridization between two strands of DNA, the complementary nature of the nucleic acid sequences specifically complementary pair hydrogen bonding between pairs of nucleotide bases to each other through the formation.

Within the liquid jet module integrated HV-ESD Clamp prospective multi-bit output integrated circuit, as shown in **Figure 22**, the DNA gene sequence of printing cards poured into 384 gates, such as nucleotide-like ink injected into specific the position of solid phase synthesis (solid phase phosphoramidite chemistry).

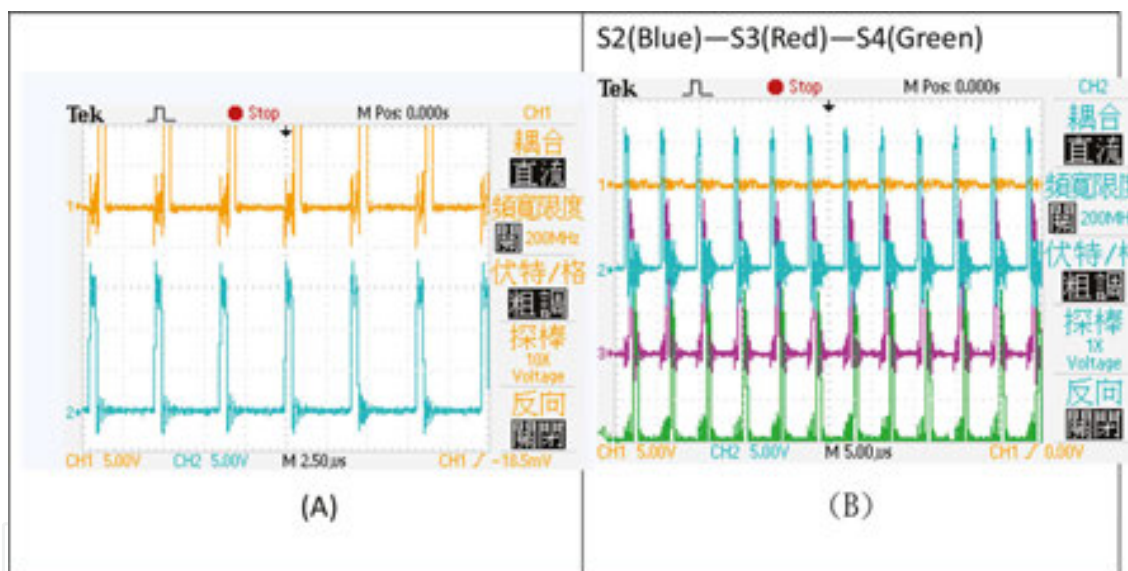


Figure 23. Two sets of data are by the AIP (PIN29) and BIP (PIN30).

The system will be open print dot DNA. It is the use of multi-circuit will print out the orifice of addressing DNA shown in **Figure 23**. There are two sets of data are by the AIP (PIN29) and BIP (PIN30) simultaneously into two 16 bits Register. With instructions sent switch control signal, each generating 384 thermal outputs. CK1 transfer instructions simultaneously send data, CK2 execute instructions simultaneously sending data to the thermal output.

ESD clamp circuit between the power (Power-Rail ESD Clamp Circuit) and inner circuit, when the electrostatic discharge protection device is used in the power supply ESD clamp device, under normal working operation, ESD protection essential element is closed. And the occurrence of electrostatic discharge when the electrostatic discharge protection device must be able

to quickly turn on to ground the electrostatic discharge current, in order to protect the internal circuit purposes as shown in **Figure 24**.

DNA droplets arrangement and detection are observation by high speed cameras. It is by the power supply, light source, liquid discharge frequency and synchronization signals to observe droplet trajectory as shown in **Figure 25**. It is modulated the observation flat-top building to a suitable position, to approve from droplet observation to catch droplet orbit phenomenon. The measurement system could calculate the droplet area, blob length, droplet injection position. **Figure 26** is shown in 5 kHz operating frequency at 30, 40 μ s injection.

Figure 27 is printed chip module photo. 50 μ m thickness of a single channel injection cavity to 5 kHz operating frequency at 10, 20, 30, 40 μ s injection is shown in **Figure 28**.

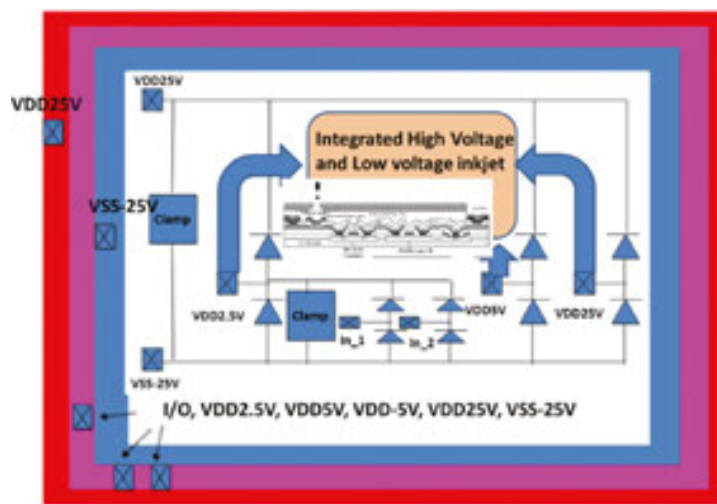


Figure 24. Thermal inkjet(TIJ) printhead with multi-level output voltage ESD protection system.

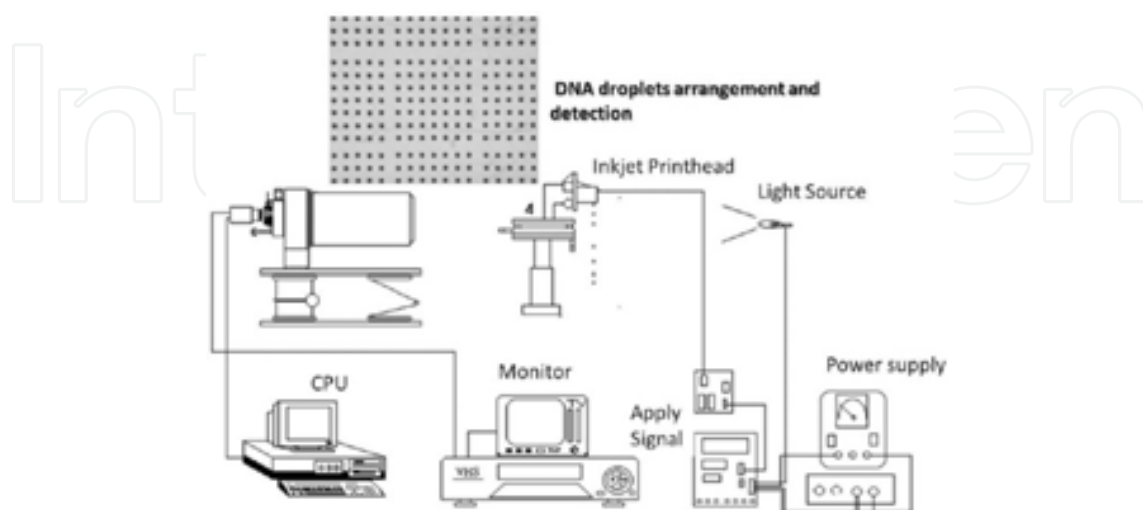


Figure 25. DNA droplets observation platform.

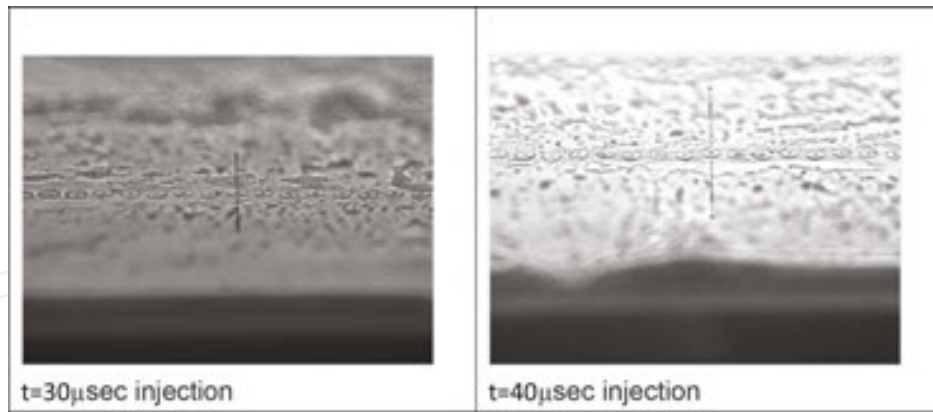


Figure 26. 5 kHz operating frequency at 30, 40 μ s injection.

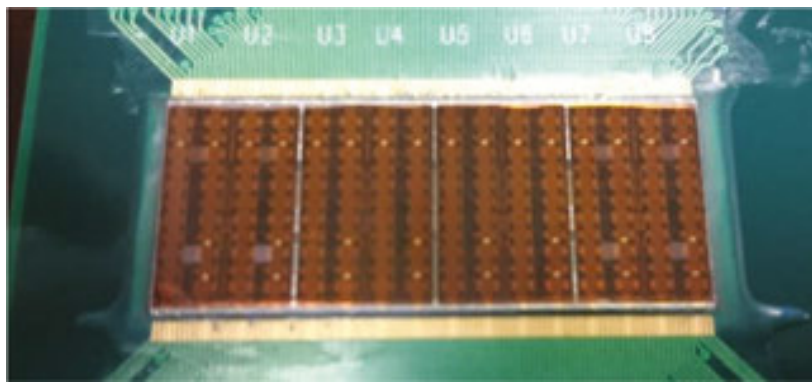


Figure 27. Printed chip module.

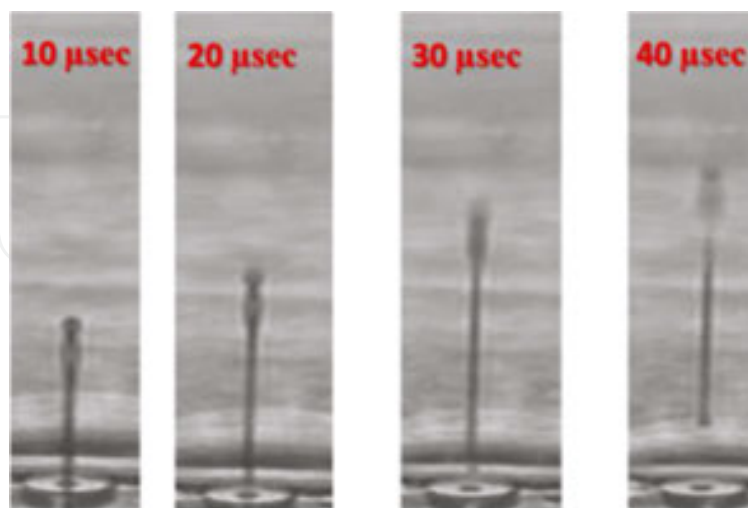


Figure 28. 5 kHz operating frequency at 10, 20, 30, 40 μ s injection.

The heated bubble manner nucleic acid probe is placed on a glass slide using a gene chip production to 30,000 points as shown in **Figure 29**. The special printing architecture method is used in system. Among them DNA time interleaving scanning sequence droplets ejection with “even group” jets, DNA droplets ejection with an addressing of two elements on the same time period driving, and DNA droplets ejection with an addressing of three elements on the same time period driving were shown in **Figure 30**. The time interleaving scanning sequence is controlled spatially on the jet elements to avoid the strong interference with DNA droplets caused by the excitation of the neighbor driven elements.

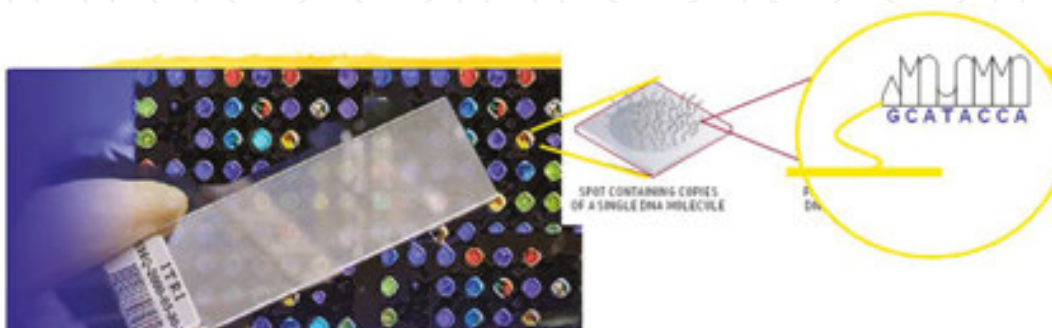


Figure 29. Nucleic acid probe placed on a glass slide.

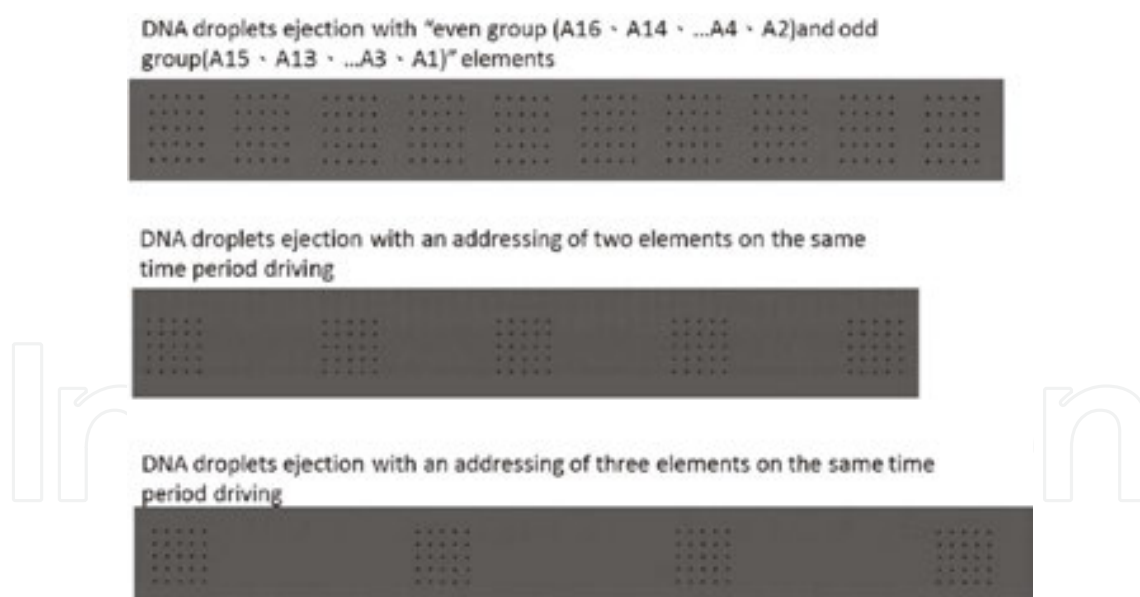


Figure 30. The special printing architecture method.

Acknowledgements

The authors acknowledge financial supports of MOST 104-2220-E-151-001.

Author details

Jian-Chiun Liou^{1,2*}

Address all correspondence to: jcliou@kuas.edu.tw

1 Department of Electronic Engineering, National Kaohsiung University of Applied Sciences (KUAS), Sanmin Dist., Kaohsiung City, Taiwan, R.O.C

2 Graduate Institute of Clinical Medicine, Kaohsiung Medical University, Taiwan, R.O.C

References

- [1] Amol A. Khalate, Xavier Bombois, Robert Babuška, Herman Wijshoff, and René Waarsing: Optimization-based feedforward control for a Drop-on-Demand inkjet printhead, American Control Conference (ACC), pp. 2182–2187(2010).
- [2] Jian-Chiun Liou, Fan-Gang Tseng: An Intelligent High-Speed 3D Data Registration Integrated Circuit Applied to Large Array Format Inkjet Printhead, NEMS '06. 1st IEEE International Conference on Nano/Micro Engineered and Molecular Systems (Zhuhai), pp. 368–372(2006).
- [3] Amol Khalate, Beno Bayon, Xavier Bombois, Gérard Scorletti, and Robert Babuška: Drop-on-demand inkjet printhead performance improvement using robust feedforward control. 50th IEEE Conference on Decision and Control and European Control Conference (CDC-ECC) (Orlando, Florida), pp. 4183–4188(2011).
- [4] S. J. Shin, K. Kuk, J. W. Shin, C. S. Lee, Y. S. Oh, and S. O. Park: Firing frequency improvement of back shooting inkjet printhead by thermal management, TRANSDUCERS. 12th International Conference on Solid-State Sensors, Actuators and Microsystems (Boston, USA), Volume: 1, pp. 380–383(2003).
- [5] Jae-Duk Lee, Choon-Sup Lee, Ki-Chul Chun, and Chul-Hi Han: Two-dimensional nozzle arrangement in a monolithic inkjet printhead for high-resolution and high-speed printing, International Electron Devices Meeting, 1999. IEDM '99. Technical Digest (Washington, DC, USA), pp.127–130(1999).
- [6] T. Goldmann and J. S. Gonzalez: DNA-printing: Utilization of a standard inkjet printer for the transfer of nucleic acids to solid supports, J. Biochem. Biophys. Methods, vol. 42, no. 3, pp. 105–110(2000).
- [7] R. Teranishi, T. Fujiwara, T. Watanabe, and M. Yoshimura: Direct fabrication of patterned PbS and CdS on organic sheets at ambient temperature by on-site reaction using inkjet printer, Solid State Ion., vol. 151, no. 1–4, pp. 97–103(2002).

- [8] T. Courtney, R.E. Drews, V. I. Hull, D. R. Ims and M.P. O'Horo: Print Element for Xerox Thermal Ink Jet Print Cartridge, in *Color Hard Copy AND Graphic Arts III*, J. Bares (Editor), Proc. SPIE, Vol. 2171, pp.126–130(1994).
- [9] P.H. Chen, W. C. Chen, and S. H. Chang: Bubble growth and ink ejection process of a thermal ink jet printhead, *Int. J. Mech. Sci.*, vol. 39, no. 6, pp.683–695(1997).
- [10] Fan-Gang Tseng, Chang-Jin Kim, and Chih-Ming Ho: A high-resolution high-frequency monolithic top-shooting microinjector free of satellite drops—Part II fabrication, implementation, and characterization, *J. of Microelectromech. Syst.*, vol. 11, no. 5, pp. 437–447(2002).
- [11] Fan-Gang Tseng, Chang-Jin Kim, and Chih-Ming Ho, A high-resolution high-frequency monolithic top-shooting microinjector free of satellite drops—Part I: Concept, design, and model, *J. Microelectromech. Syst.*, vol. 11, no. 5, pp. 427–436(2002).
- [12] C. T. Pan, J. Shiea, and S. C. Shen: Fabrication of an integrated piezoelectric micro-nebulizer for biochemical sample analysis, *J. Micromech. Microeng.*, vol. 17, no. 3, pp. 659–669, Mar. 2007.
- [13] S. C. Tzeng and W. P. Ma: Study of flow and heat transfer characteristics and LIGA fabrication of microspinnerets, *J. Micromech. Microeng.*, vol. 13, no. 5, pp. 670–679(2003).
- [14] J.H. Park, and Y.S. Oh: Investigation to minimize heater burnout in thermal thin film print heads, *Microsystem Technologies*, vol. 11, Berlin: Springer, pp. 16–22(2005).
- [15] C.M. Chang, I.D. Yang, R. J. Yu, Y. L. Lin, F. G. Tseng, and C. C. Chieng, *Inkjet Printhead Arrays with No Separating Wall Between Bubbles: Solid-State Sensors, Actuators and Microsystems Conference (Lyon)*, pp. 175–178(2007).
- [16] T. G. Kang et al.: A four-bit microinjector using microheater array for adjusting the ejected droplet volume, *IEEE JMEMS*, vol. 14, pp. 1031–1038(2005).
- [17] Sheng-Chih Shen, Min-Wen Wang, and Chung-Jui Lee: Manufacture of an integrated three-dimensional structure nozzle plate using microinjection molding for a 1200-dpi inkjet printhead, *J. Microelectromech. Syst.*, vol. 18, no. 1, pp. 52–63(2009).
- [18] F. Takagi, R. Kurosawa, D. Sawaki, S. Kamisuki, M. Takai, K. Ishihara, and M. Atobe: Pico liter dispenser with 128 independent nozzles for high throughput biochip fabrication, *17th IEEE International Conference on Micro Electro Mechanical Systems, 2004. (MEMS) (Netherlands)*, pp. 276–279(2004).
- [19] Ji-Hyuk Lim, Keon-Kuk, Seung-Joo Shin, Seog-Soon Baek, Young-Jae Kim, Jong-Woo Shin, and Yong-Soo Oh: Investigation of reliability problems in thermal inkjet printhead, *IEEE International Reliability Physics Symposium Proceedings (Phoenix, Arizona)*, pp. 251–254(2004).

- [20] T. Lindemann, H. Ashauer, Ying Yu, D.S. Sassano, Roland Zengerle, and P. Koltay: One inch thermal bubble jet printhead with laser structured integrated polyimide nozzle plate, *J. Microelectromech. Syst.*, vol. 16, pp. 420–428(2007).
- [21] A. van der Bos, T. Segers, R. Jeurissen, M. van den Berg, H. Reinten, H. Wijshoff, M. Versluis, and D. Lohse: Infrared imaging and acoustic sizing of a bubble inside a micro-electro-mechanical system piezo ink channel, *J. Appl. Phys.*, vol. 110, no. 3, pp. 034503–034503-7(2011).
- [22] M. Einat, and M. Grajower: Microboiling Measurements of thermal-inkjet heaters, *J. Microelectromech. Syst.*, vol. 19, no. 2, pp. 391–395(2010).
- [23] S.J. Shin, K. Kuk, J.W. Shin, C.S. Lee, Y.S. Oh, and S.O. Park: Firing frequency improvement of back shooting inkjet printhead by thermal management, 12th International Conference on TRANSDUCERS, Solid-State Sensors, Actuators and Microsystems (Boston, USA), Volume: 1, pp.380–383 (2003).